Article

Evaluation of Fuel Gas Supply System for Marine Dual-Fuel Propulsion Engines Using LNG and Ammonia Fuel

Soobin Hyeon [iD], Jinkwang Lee [iD] and Jungho Choi *[iD]

Department of Naval Architecture and Offshore Engineering, Dong-A University, 37 Nakdong-daero 550 Beon-gil, Saha-gu, Busan 49315, Korea
* Correspondence: tamuchoi@dau.ac.kr; Tel.: +82-51-200-7938

Abstract: This study proposes a fuel supply system for dual-fuel propulsion engines using liquefied natural gas (LNG) and ammonia to control carbon emissions. The independent fuel supply system of LNG and ammonia is configured as a hybrid system. The operating pressure of the re-condenser is determined as a process variable according to the power consumption and flow rate of the non-condensable boil-off gas. The independent and hybrid systems are compared and evaluated through thermodynamic analyses, including specific power consumption (SPC) and exergy analyses, with respect to the fuel ratio and engine load. When the engine load is 100% in Case 1 for a 40% carbon reduction by 2030, the hybrid system exhibits an SPC reduction of 70% and exergy efficiency increase of 16% compared with the independent system.

Keywords: fuel gas supply system; dual-fuel engine; LNG; ammonia; exergy analysis; specific power consumption

1. Introduction

At the International Maritime Organization (IMO) meeting in April 2018, it was agreed to reduce carbon dioxide (CO_2) emissions by 40% by 2030 and by >70% by 2050, compared with the level in 2008 [1]. Corresponding measures include energy efficiency improvement, hull form improvement, carbon capture and storage, and the application of eco-friendly fuels. Among them, the application of eco-friendly fuels achieves the most significant reduction in carbon emissions [2]. LNG, a low-carbon fuel, has been commercialized as a fuel for ships and can reduce CO_2 emissions by 20% compared to heavy fuel oil (HFO) [3]. Because strict IMO regulations can be satisfied by using carbon-free fuels, such as hydrogen and ammonia, the use of carbon-free fuels is necessary to reduce CO_2 emissions.

Hydrogen has the advantage of producing heat and electrical energy, with water as the only byproduct; however, its combustion rate is high, which may lead to the flashback phenomenon [4]. Additionally, the storage of liquefied hydrogen is technically tricky owing to its low boiling point of only 19 K at atmospheric pressure. Potential safety issues arise from the low flash point and the absence of visible flames [5,6]. Ammonia has attracted attention as a carbon-free fuel because it does not generate CO_2 during combustion and has a relatively high boiling point of 240.15 K at atmospheric pressure, which facilitates storage [6]. In addition, the cost per volume of energy storage is three times lower than that for hydrogen [7]. However, the application of ammonia as the primary fuel to replace HFO is bound because of the ignition issue caused by its low heating value and high auto-ignition temperature [8].

Various methods have been investigated to improve the combustion properties of ammonia. Among these, the dual-fuel method of mixing ammonia with LNG, which has been commercialized as a ship fuel, has attracted interest in overcoming the combustion limitations of ammonia. Ishikawajima-Harima Heavy Industries Co., Ltd. developed a gas turbine using LNG and ammonia and proposed a critical fuel supply system [9]. Further,

Maschinenfabrik Augsburg-Niernberg aims to develop a two-stroke ammonia engine by 2024 and is designing the necessary ammonia supply system based on the LPG supply system [10]. The China State Shipbuilding Corporation is also developing a system to supply high-pressure liquid ammonia to engines [11]. For ammonia dual-fuel engines, Oh et al. investigated the combustion potential of a dual-fuel engine using LNG and ammonia. They measured the CO_2 emissions for the air–fuel ratio and fuel fraction. CO_2 emissions were reduced by 28% by replacing LNG with ammonia by 50% (by volume) [12]. Reiter et al. identified a dual-fuel engine's combustion and exhaust characteristics at various mixing ratios of ammonia and diesel fuel. Furthermore, he found that an increase in the ammonia extended the ignition delay and reduced the peak combustion pressure. In addition, although NO emissions increased with the ammonia mixing ratio, there was no problem as long as ammonia accounted for <40% of the total flow rate [13].

A fuel gas supply system (FGSS) that supplies fuel according to engine requirements is required to use the LNG fuel [14]. Various studies on LNG FGSSs have been conducted for LNG propulsion ships. Seo et al. proposed a new system for supplying LNG to an engine without a pump and compared the cost over the lifespan with that of a system with a pump [15]. Lee et al. calculated the flow rate and power consumption of the utility system according to the mixing ratio of water and glycol used to vaporize LNG in the FGSS; they found that the flow rate and power consumption increased compared with the case where only water was used [16]. Wang et al. performed a lifecycle cost evaluation of an FGSS for different boil-off gas (BOG) processing methods, considering the ship size, sailing time, LNG fuel price, and lifespan, and proposed a strategy for FGSS arrangement based on the evaluation results. Re-liquefying BOG on the ship was found advantageous in the case of a short sailing time and high LNG price, whereas supplying BOG as fuel for the auxiliary engine was found economical in the case of a long sailing time and low LNG price [17]. Kim et al. conducted an economic evaluation considering whether a BOG re-liquefaction facility was installed in an FGSS for high-pressure fuel. The annual cost decreased with the installation of a BOG re-liquefaction facility when the LNG price was ≥5 USD/MMBtu, whereas combustion was more economical when the LNG price was ≤4 USD/MMBtu [18].

Studies have been performed on the development of LNG and ammonia FGSSs, BOG processing systems of LNG propulsion ships, and characteristics of dual-fuel engines using LNG and ammonia. However, there is a lack of studies on the technology development and FGSSs for dual-fuel engines using LNG and ammonia. Therefore, an FGSS was developed and evaluated for dual-fuel engines using LNG and ammonia in this study. An independent system comprising conventional LNG and ammonia fuel supply systems and a hybrid system combining the two systems were evaluated. Significantly, the devised hybrid system has the characteristics of efficiently processing the BOG of the LNG fuel by adopting a re-condenser for LNG and processing the BOG of the ammonia fuel by utilizing LNG cooling energy. Furthermore, the systems were designed to control the 2030 and 2050 carbon dioxide reduction with ammonia amount while using LNG as the main fuel. These systems were evaluated through thermodynamic analyses, the specific power consumption (SPC) and exergy efficiency.

2. Methods

In this study, the systems were analyzed according to the system arrangement, mixed amounts of LNG and ammonia (which were based on the goal of carbon reduction), and engine load. The system arrangement was compared between the independent and hybrid systems. Herein, the mixing ratio of LNG and ammonia for a 40% carbon reduction by 2030 is derived in Case 1, and that for a 70% carbon reduction by 2050 is studied in Case 2.

2.1. System Description

This study targeted a 15,000-TEU container ship operating on LNG and ammonia fuel, and the LNG tank was designed according to the 12,000 m³ membrane atmosphere type. The boil-off rate (BOR) of the LNG tank was 0.15%/d, and the BOG amount was

calculated based on the BOR [19]. When the mixing ratio of ammonia and LNG was 50%, the tank size for the ammonia fuel was estimated to be 6630 m^3 with a 100% margin taken into consideration under the assumption that the ship would be operated for 15 days. The heat influx was computed under the assumption that the insulation material of the tank consisted of 120-mm-thick polyurethane foam (k = 0.021 W/(m·K)), and the BOG amount was figured accordingly.

The supply flow rate was determined by selecting the engine model for the existing 15000-TEU container ship, and the propulsion engine consisted of four Wartsila 16V46DF units. The fuel supply conditions were based on previous experimental studies involving LNG and ammonia dual-fuel engines. Table 1 lists the inlet and outlet boundary conditions of the systems [12].

Table 1. System boundary conditions.

	LNG	Ammonia	Glycol Water (G/W)
Composition (mole%)	CH_4: 0.94 C_2H_6: 0.47 C_3H_8: 0.008 C_4H_{10}: 0.002 N_2: 0.003	Ammonia: 1	Ethylene glycol: 0.5 H_2O: 0.5
Tank capacity (m^3)	12,000	6630	-
Storage pressure (kPa)	101.3	101.3	-
Storage temperature (K)	110.15	240.15	-
Supply pressure (kPa)	800	450	500
Supply temperature (K)	313.15	313.15	323.15

Modeling was performed with the commercial process simulation program Aspen HYSYS V11, and the Peng–Robinson equation was adopted as the equation of state. The following assumptions were made for the modeling.

- The composition of the BOG of LNG is identical to that of LNG.
- The amount of BOG is determined based on the amount of fuel (85 vol.%) loaded in the tank.
- LNG, ammonia, and BOG are supplied in a saturated state.
- The minimum temperature approach of the heat exchanger was 10 K.
- The pressure losses on the tube side and the shell side of the heat exchanger are 68.95 and 34.47 kPa, respectively.
- The temperature of ammonia after heat exchange is set at 228.15 K, considering the freezing point at atmospheric pressure (196.15 K).
- Pressure loss in the pipes is not considered.
- The efficiency of the compressors and pumps is 75%.
- Chemical exergy is not considered.

2.1.1. Independent System

Figure 1a,b show the FGSSs for LNG and ammonia engine supplies from previous studies, respectively [9–11]. In the LNG FGSS, LNG is delivered through a pump (LNG PP) in a tank operating at atmospheric pressure and then introduced into a vaporizer (LNG-G/W HEX). LNG is vaporized by G/W as a heat source in the vaporizer (LNG-G/W HEX), heated by a heater (NG heater) to the temperature required for the engine (313.15 K), and supplied to the main propulsion engine. The BOG generated from the fuel LNG fuel tank is compressed and cooled to control the tank pressure and be used as fuel for the auxiliary engine.
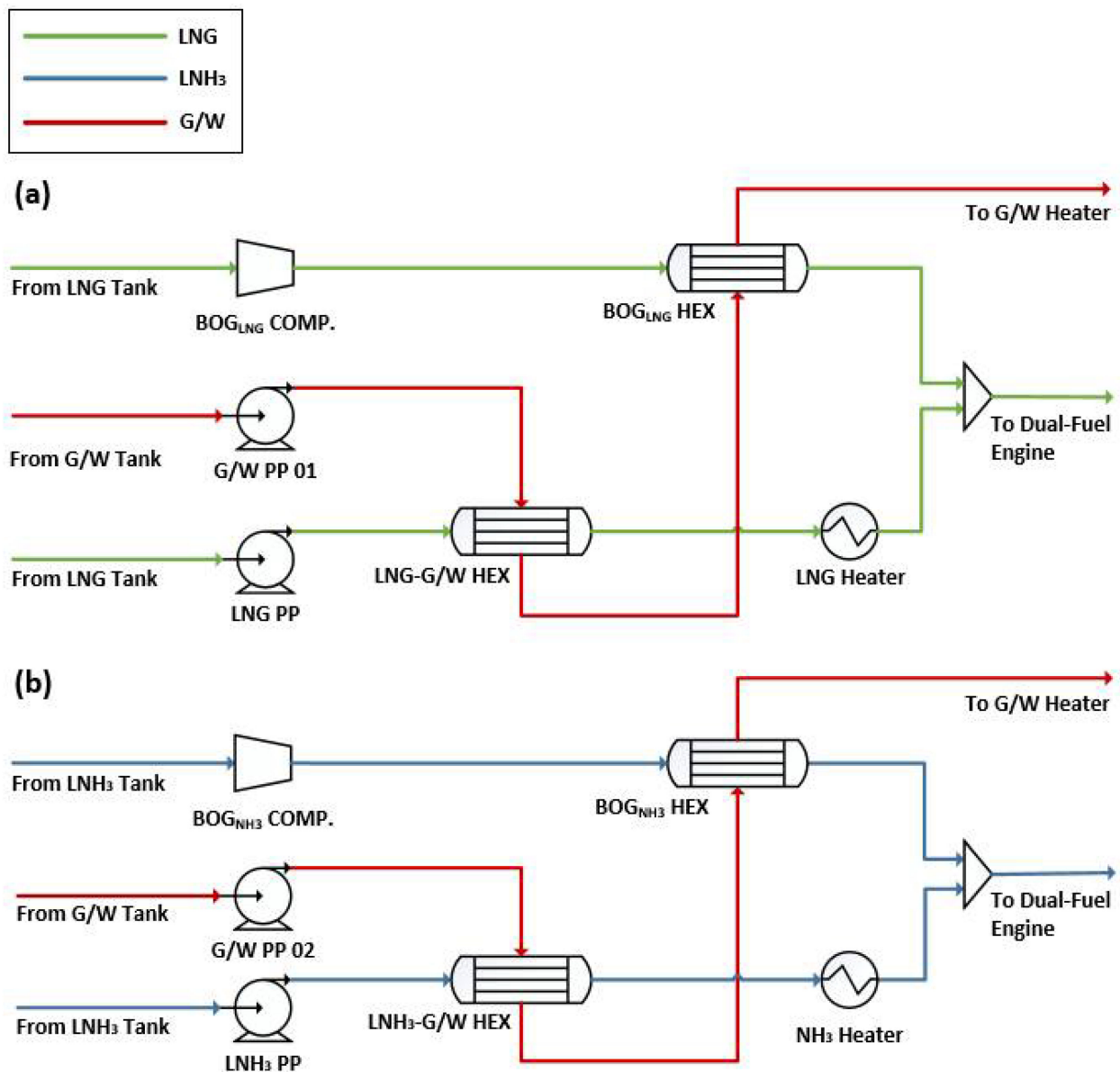
Figure 1. Schematics of the conventional independent FGSSs: (**a**) LNG; (**b**) ammonia.

The system configuration of the ammonia FGSS is similar. The fuel in the tank is transferred through a pump (LNH$_3$ PP) and introduced into a vaporizer (LNH$_3$-G/WHEX). Next, ammonia is vaporized with G/W in the vaporizer (LNH$_3$-G/WHEX) and is supplied as fuel. After the heat exchange with ammonia, G/W undergoes another heat exchange in the heat exchanger (BOG$_{LNH3}$ HEX) to cool the compressed BOG$_{NH3}$ to a low temperature.

2.1.2. Hybrid System

In this study, an FGSS for dual-fuel engines was developed by configuring the independent FGSSs for LNG and ammonia into a hybrid form, as shown in Figure 2. The FGSS in hybrid form consists of a BOG re-condensing section, fuel vaporization section, and utility section. In the conventional system, the BOG from the fuel tank is compressed into a gaseous state and used as fuel. In contrast, in the proposed system, because compressing the gaseous BOG requires a large amount of power, the BOG is re-condensed with LNG cold energy to be sent back to the tank or used as fuel.
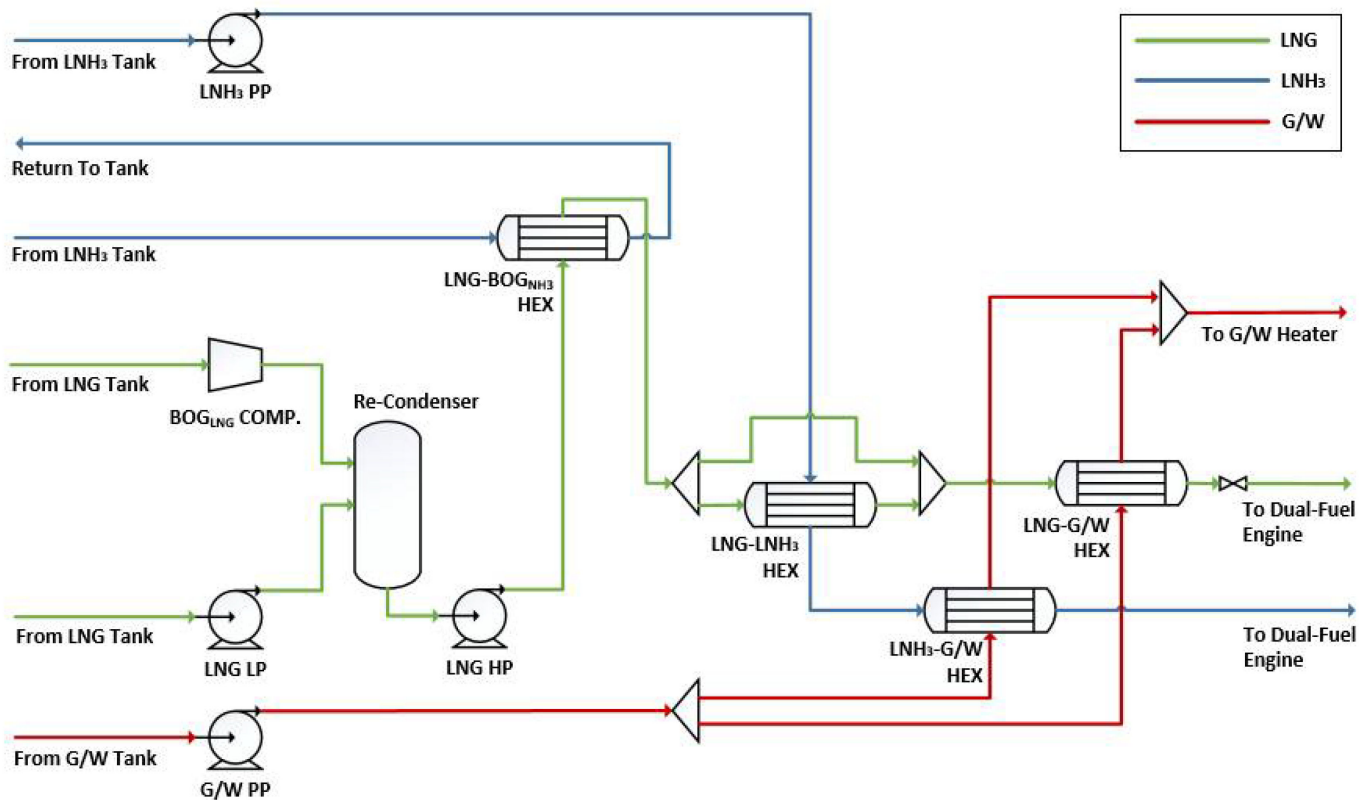
Figure 2. Schematic of the hybrid FGSS.

BOG_{LNG} is first compressed using a compressor (BOG_{LNG} COMP) and subsequently re-condensed through RE-CONDENSER using compressed LNG in a subcooled liquid state [20]. In this case, the compression pressure is the minimum pressure at which the BOG_{LNG} is 100% re-condensed, and the pressure increases as the flow rate of the LNG decreases. LNG discharged from the RE-CONDENSER increases the pressure in the LNG HP and attains a subcooled state. Subsequently, LNG in the subcooled state is supplied to the heat exchanger (LNG-BOG_{NH3} HEX) for re-liquefaction through heat exchange with BOG_{LNH3} and recovered into the tank.

After the heat exchange, LNG flows into the heat exchanger (LNG-LNH_3 HEX) to exchange heat with ammonia. Before ammonia and LNG exchange heat with G/W, the temperature of the LNG increases with ammonia, and LNG is vaporized through heat exchange with G/W. Because the ammonia freezing issue can happen if the LNG flow rate for heat exchange with ammonia is 100%, some LNG bypasses the heat exchanger to avoid the freezing problem. To satisfy the temperature required for the engine (313.15 K), LNG and ammonia exchange heat with G/W at the LNG-G/W HEX and LNH_3-G/W HEX.

In the conventional independent fuel supply system, each fuel is vaporized using G/W; however, in the hybrid fuel supply system, the heat source of ammonia is used to increase the temperature of the LNG, and G/W is used to compensate for an insufficient heat source. Consequently, the power consumption is reduced by reducing the G/W flow rate.

2.2. LNG and Ammonia Mixing Ratio

The LNG and ammonia flow rates required to realize the carbon-neutral target of the IMO for the shipping industry were calculated. Although the use of LNG as fuel reduces carbon emissions by approximately 20% compared with HFO, CO_2 emissions must be reduced further by mixing ammonia to achieve carbon neutrality goals of 40% and 70% carbon reductions by 2030 and 2050, respectively, compared to 2008 [3]. Carbon emissions are computed according to the amount of carbon generated during LNG combustion,

and Equations (1)–(4) are the combustion reaction equations for the main hydrocarbon components of LNG, excluding nitrogen (N_2): methane (CH_4), ethane (C_2H_6), propane (C_3H_8), and butane (C_4H_{10}) [20].

$$CH_4 + 2O_2 \rightarrow CO_2 + 2H_2O \tag{1}$$

$$2C_2H_6 + 7O_2 \rightarrow 4CO_2 + 6H_2O \tag{2}$$

$$C_3Hg + 5O_2 \rightarrow 3CO_2 + 4H_2O \tag{3}$$

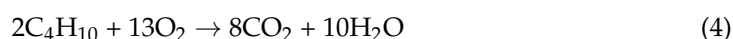$$2C_4H_{10} + 13O_2 \rightarrow 8CO_2 + 10H_2O \tag{4}$$

Table 2 presents the mass flow rates of the two fuels calculated by determining the maximum LNG flow rate satisfying Cases 1 and 2 and substituting ammonia for insufficient energy for engine power.

Table 2. Mass flow rates of LNG and ammonia at different engine loads.

System		Independent System				Hybrid System			
Case		Case 1		Case 2		Case 1		Case 2	
Mass flow rate (kg/h)		LNG	Ammonia	LNG	Ammonia	LNG	Ammonia	LNG	Ammonia
Engine load	50%	3123	2771	1561	6924	3124	2768	1562	6924
	75%	4657	4131	2328	10,324	4659	4127	2329	10,323
	100%	6191	5491	3095	13,724	6193	5487	3096	13,722

2.3. Optimized Pressure Selection Method for Hybrid System

Among the components of the hybrid system, RE-CONDENSER re-condenses BOG_{LNG} to LNG in a subcooled liquid state, during which the compression pressure varies with respect to the LNG flow rate [21]. This is because the amount of energy held by the LNG and BOG_{LNG} of the LNG should be identical during re-condensation, and a sufficient flow rate of LNG reduces the compression pressure of the BOG_{LNG}, which allows re-condensation even with a significant latent heat interval. Conversely, when the LNG flow rate is low, re-condensation is possible with a small amount of LNG by compressing BOG_{LNG} and reducing the latent heat interval. Therefore, the pressure required for the complete re-condensation of BOG_{LNG} varies for the LNG flow rate.

Because the compressor discharge pressure affects the system efficiency, the optimal operating pressure of RE-CONDENSER was determined by the power consumption and flow rate of the non-condensed BOG of the LNG at different discharge pressures of BOG_{LNG} COMP and LNG LP. The compression pressure ranges from 150 to 2500 kPa, and the power consumption in the system increases as the pressure increases. However, when the compression pressure is too low, the amount of BOG that can be condensed in RE-CONDENSER decreases, thus necessitating appropriate pressure control.

2.4. System Evaluation Method
2.4.1. Specific Power Consumption

As the required flow rate changes of the engine, the mixing ratio of LNG and ammonia varies between the cases; consequently, the power consumption of the two fuel supply systems changes. For the independent system, power varies only with respect to the flow rate; however, for the hybrid system, power varies with the changing compression pressure of the re-condensing system. Therefore, the SPC is compared between the systems

according to the engine load and case. Equation (5) shows The SPC's definition, dividing the power consumption by the supply rates of LNG and ammonia as follows [22].

$$\text{SPC(kWh/kg)} = \frac{Power}{\dot{m}}. \tag{5}$$

2.4.2. Exergy Theory

Exergy flow is defined as the maximum effective energy obtained from a stream when the equilibrium state is reached through interaction in the standard environment in Equation (6) [23].

$$\dot{E}_x = \dot{m}e_x = \dot{m}[(h_1 - h_0) - T_0(s_1 - s_0)], \tag{6}$$

where h_1 and s_1 represent the enthalpy and entropy in State 1, respectively, and subscript 0 indicates the standard environmental conditions (1 atm and 25 °C).

Table 3 presents the equations for calculating the exergy destruction and efficiency of each equipment unit [24]. Exergy destruction refers to the irreversible loss of energy, such as friction loss, within a test volume [25]. This study evaluated and compared the exergy destruction and efficiency of an independent system, a hybrid system, and each piece of equipment.

Table 3. Equation of exergy destruction and efficiency of the components.

Equipment	Exergy Destruction (kW)	Exergy Efficiency (%)
Pump, compressor	$\dot{Ex}_{in} + \dot{W}_{in} - \dot{Ex}_{out}$	$\frac{\dot{Ex}_{out} - \dot{Ex}_{in}}{\dot{W}_{in}}$
Heater	$\dot{Ex}_{in} + \dot{Q}_{in} - \dot{Ex}_{out}$	$\frac{\dot{Ex}_{out} - \dot{Ex}_{in}}{\dot{Q}_{in}}$
Separator, tee, mixer, and heat exchanger	$\dot{Ex}_{in} - \dot{Ex}_{out}$	$\frac{\dot{Ex}_{out}}{\dot{Ex}_{in}}$

3. Results

3.1. Optimized Pressure Selection for Hybrid System

Because the mixing ratio of LNG and ammonia varied for the engine load in each case, the following results were obtained to investigate the effect of the re-condensing system.

Figure 3a,b illustrates the power consumption of the systems according to the engine load and flow rate of the non-condensable BOG of the LNG at RE-CONDENSER in Cases 1 and 2. As the engine load increased to 50%, 75%, and 100%, the supply flow rate increased, and the overall power consumption increased. Additionally, because the operating pressure of RE-CONDENSER to fully re-condense the BOG became lower at a higher LNG flow rate, the power consumption decreased with an increase in engine load. Table 4 shows the minimum pressures at which the BOG was completely re-condensed.
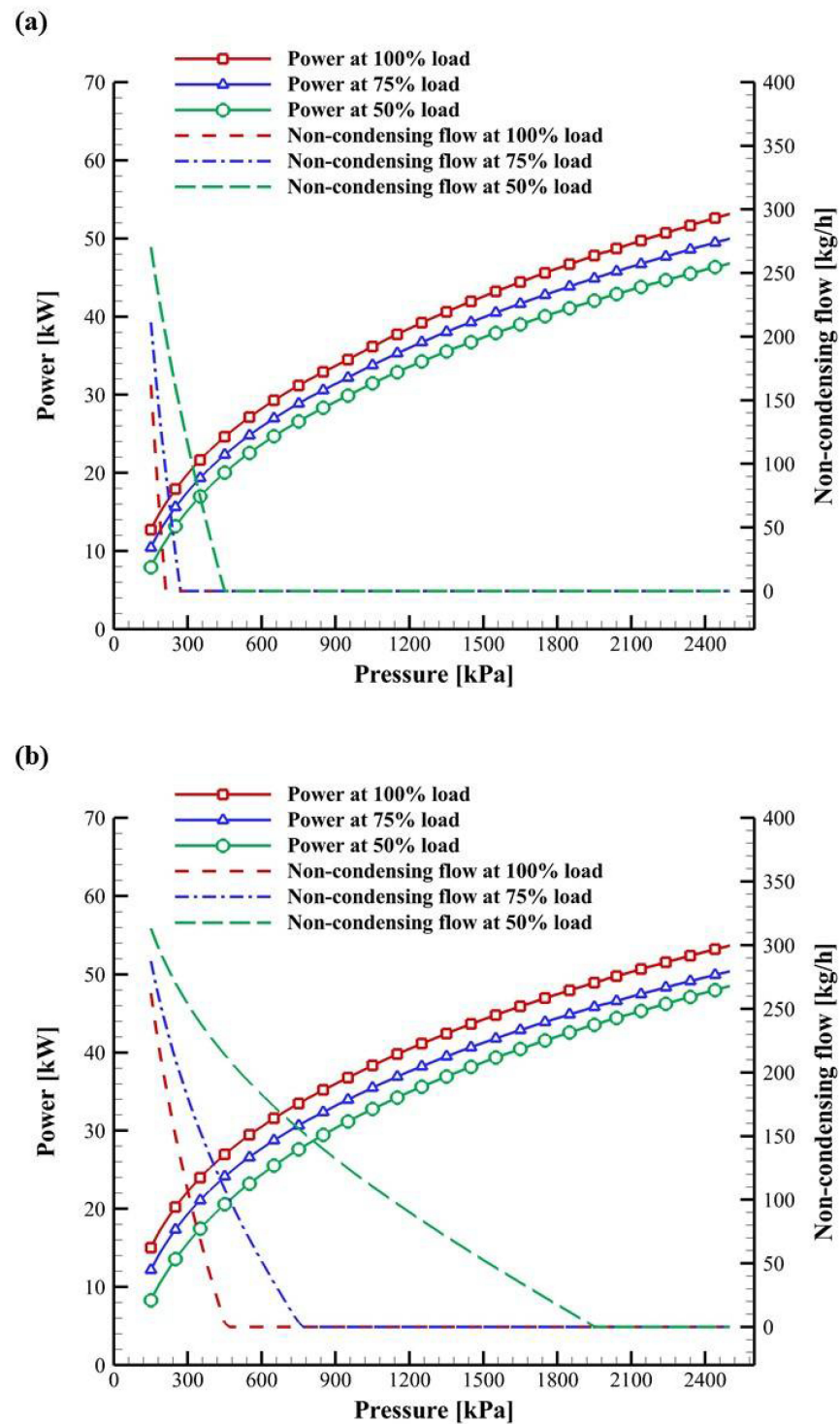
Figure 3. Power requirements and non-condensing flow with respect to the compression pressure: (**a**) Case 1; (**b**) Case 2.

Table 4. Optimized pressure for the hybrid system.

Case	50% Load	75% Load	100% Load
Case 1	449 kPa	273 kPa	211 kPa
Case 2	1953 kPa	762 kPa	371 kPa

3.2. Energy Efficiency

As shown in Figure 4, SPC was compared between the independent and hybrid systems at an engine load of 100%. In Cases 1 and 2, the SPC was reduced by 69% and 57%, respectively, for the hybrid system compared with the independent system, which indicates that the power consumption of the system was reduced. In addition, the SPC of the hybrid system was higher in Case 2 than in Case 1. Because the LNG flow rate was lower in Case 2, the compression pressure required to completely re-condense the BOG had to become higher, leading to increased power consumption.
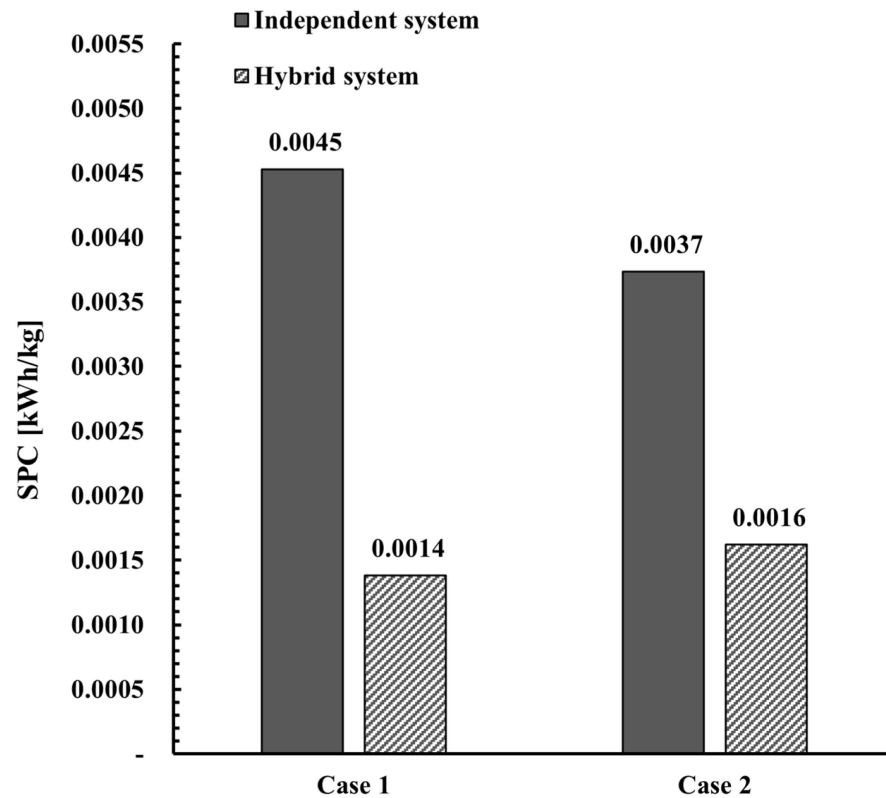

Figure 4. Specific power consumption for the different system configurations.

Case Study

Correlations between the power consumption and SPC for the independent and hybrid systems in the two cases were examined using the engine load as a process variable.

Figure 5a shows the power consumption of the independent system in each case. The system consists of a pump for each type of fuel, a BOG compressor, and a G/W pump; the BOG compressor accounts for the largest proportion of the power consumption. However, the BOG compressor is supplied at a constant flow rate and pressure even when the engine load changes. Hence, power consumption does not vary with respect to the engine load, and the fuel and G/W pumps influence the dependence of the power consumption on the engine load. Therefore, as the engine load increased, the supply flow rate and the power consumption of the fuel and G/W pumps increased, increasing the overall power consumption of the system.
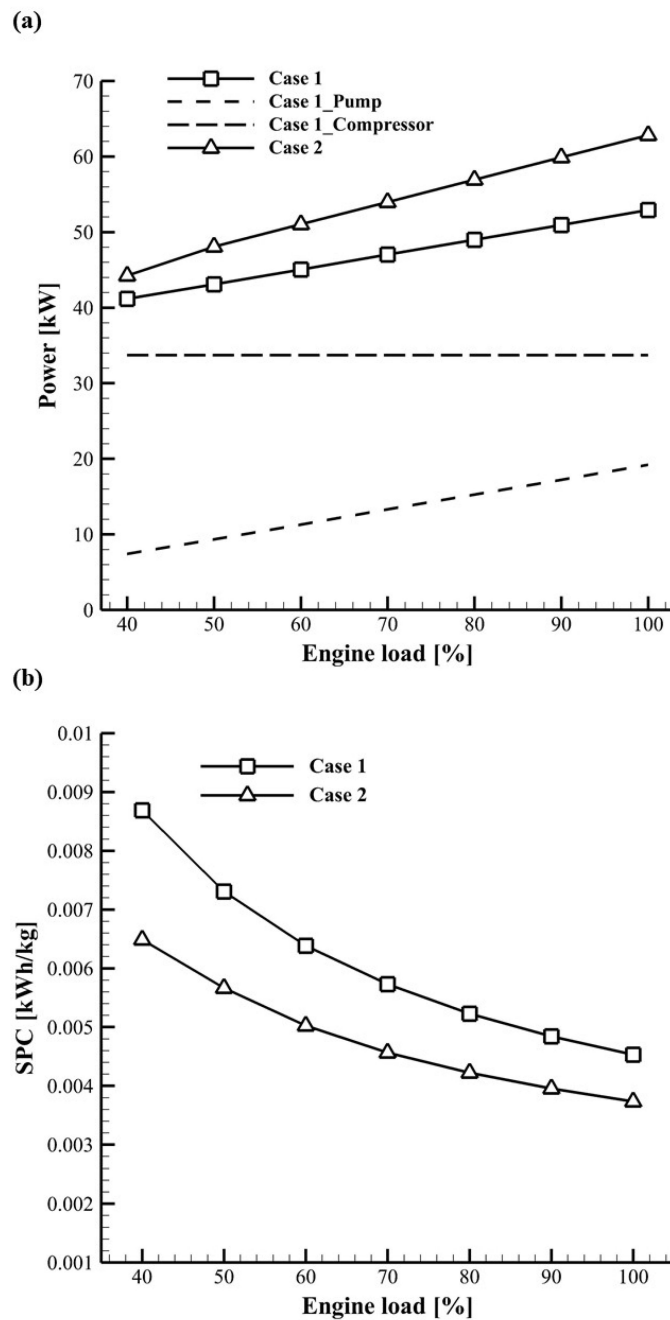
(a)

(b)

Figure 5. Energy efficiency with respect to the engine load for the independent system: (**a**) power consumption; (**b**) SPC.

Figure 5b shows the SPC of the independent system. As the engine load increased, the overall power consumption of the system increased, and the SPC decreased. Because the power consumption of the BOG compressor, which accounted for the largest proportion of the total power consumption of the system, remained constant, the efficiency increased despite the increased flow rate and power consumption.

Figure 6a shows the power consumption of the hybrid system, which was affected by the compressor and pump in the re-condensing section, fuel supply pump, and G/W pump. As the engine load increased, the flow rate and power consumption increased for the equipment required to supply fuel, whereas the pressure required for re-condensing the BOG_{LNG} decreased, thus reducing the amount of power needed for re-condensation. Power consumption of the re-condensing equipment accounted for a larger proportion of

the total power consumption of the system than that of the fuel supply pump and G/W pump, and it tended to decrease as the engine load increased. In addition, the power consumption in Case 2 exceeded that in Case 1; with the strict carbon emission reduction target, the LNG flow rate decreased, whereas that of ammonia increased, which increased the compression pressure of the re-condensing system.
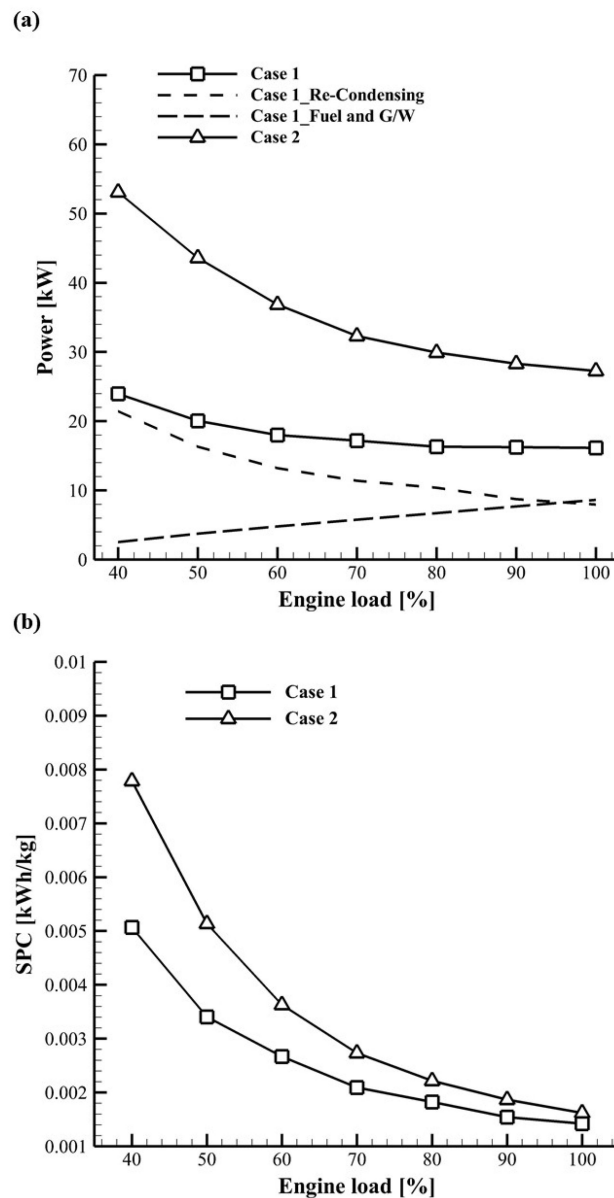

Figure 6. Energy efficiency of the hybrid system with respect to the engine load: (**a**) power consumption; (**b**) SPC.

Figure 6b shows the SPC of the hybrid system. The trend is similar to that of power consumption as the engine load increased, and the change in the SPC was larger in Case 2 than in Case 1, owing to the higher mixing ratio of ammonia.

3.3. Exergy Efficiency

The power consumption, exergy destruction, and exergy efficiency of the conventional independent system and proposed hybrid system were analyzed according to the carbon-neutrality targets in Cases 1 and 2.

Figure 7 shows the exergy destruction and efficiency of the independent and hybrid systems in Cases 1 and 2. Compared with the independent system, the exergy destruction of the hybrid system was reduced by 14% and 25% and the exergy efficiency was increased by 16% and 22% for Cases 1 and 2, respectively. These results were affected by the change in exergy for each equipment unit, as shown in Tables 5–7.
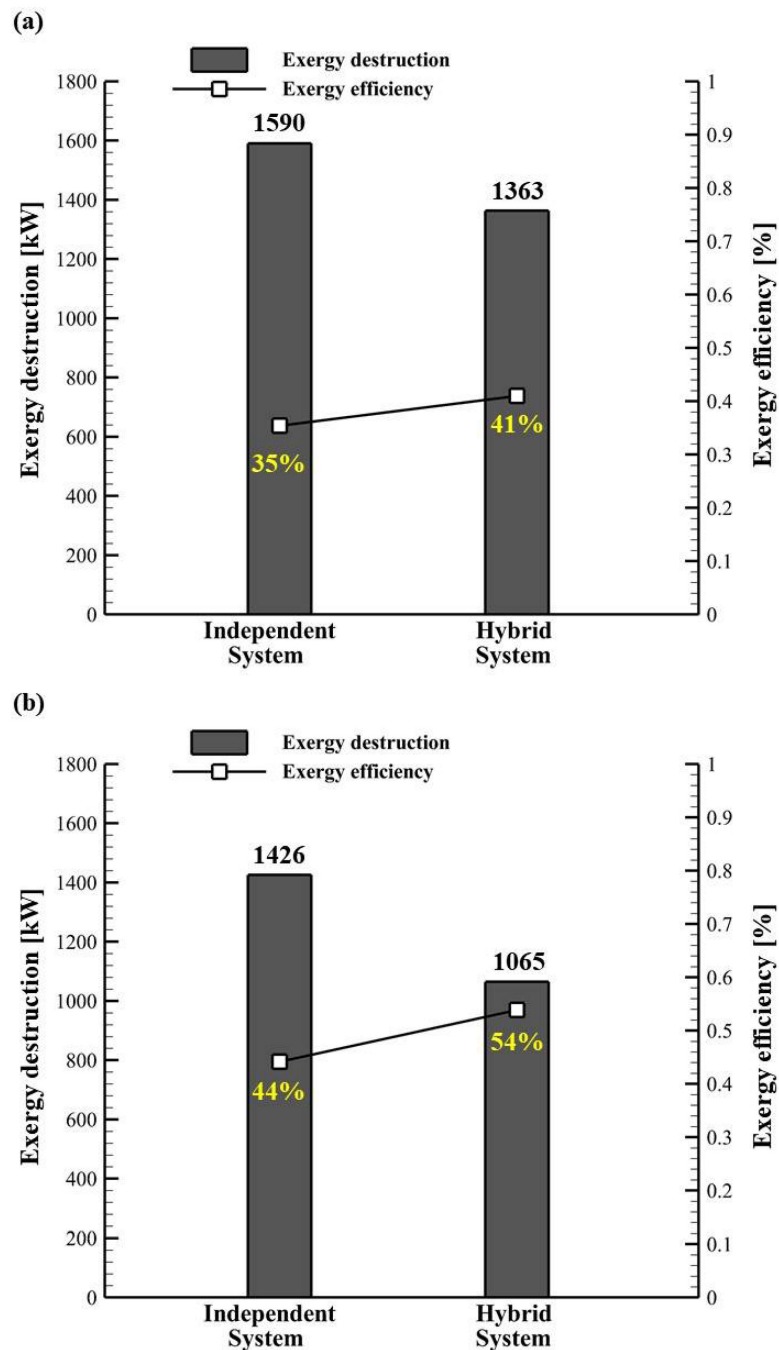

Figure 7. Exergy destruction and efficiency for the different system configurations: (**a**) Case 1; (**b**) Case 2.

Table 5. Exergy destruction and efficiency of compression equipment.

Equipment for Independent System	Exergy Destruction (kW)	Exergy Efficiency	Equipment for Hybrid System	Exergy Destruction (kW)	Exergy Efficiency
LNG PP	3.5	100%	LNG LP	0.5	100%
BOG_{LNG} COMP.	5.9	80%	BOG_{LNG} COMP.	2.7	81%
LNH_3 PP	0.3	100%	LNG HP	3.1	100%
BOG_{NH3}COMP.	2.1	80%	LNH_3 PP	0.3	100%
G/W PP 01	0.0	100%	G/W PP	0.0	100%
G/W PP 02	0.0	100%	-	-	-

Table 6. Exergy destruction and efficiency for the heat exchanger and heater.

Equipment for Independent System	Exergy Destruction (kW)	Exergy Efficiency	Equipment for Hybrid System	Exergy Destruction (kW)	Exergy Efficiency
LNG-G/W HEX	1232	30%	LNG-LNH_3 HEX	60	96%
NG heater	20	96%	LNG-LNH_3 HEX	55	92%
BOG_{NG} HEX	3	93%	LNG-G/W HEX	974	36%
LNH_3-G/W HEX	286	56%	LNH_3-G/W HEX	228	63%
LNH_3 heater	33	91%	-	-	-
BOG_{NH3} HEX	4	85%	-	-	-

Table 7. Exergy destruction and efficiency for other equipment.

Equipment for Independent System	Exergy Destruction (kW)	Exergy Efficiency	Equipment for Hybrid System	Exergy Destruction (kW)	Exergy Efficiency
MIX 01	0.5	100%	RE-CONDENSER	20.9	99%
MIX 02	0.0	100%	TEE 01	0.0	100%
-	-	-	MIX 01	18.1	99%
-	-	-	TEE 02	0.0	100%
-	-	-	MIX 02	0.0	100%
-	-	-	VLV 01	0.0	100%

Table 5 presents a comparison of the exergy destruction and efficiency of the compression equipment between the independent and hybrid systems. For the LNG and G/W pumps, the exergy destruction and efficiency did not significantly differ because they handle incompressible fluids. In the independent system, there are BOG compressors for both LNG and ammonia to use the BOG generated from the tank directly as fuel, which involves high power consumption because the BOG is compressed in accordance with the engine requirements. For the hybrid system, the BOG generated in the ammonia tank is re-liquefied through heat exchange with LNG, which requires no compressor. Whereas the BOG in the LNG tank requires a compressor for re-condensation; however, the power consumption is insignificant because the compression pressure is low. A comparison of the BOG compressors between the two systems indicated that the total exergy destruction of the compressor of the hybrid system was reduced by 66% compared with that of the independent system.

Table 6 describes a comparison of the exergy destruction and efficiency of the heat exchanger and heater. As the independent system vaporized LNG and ammonia using G/W without a preheating process, the difference between the inlet and outlet temperatures of the heat exchanger was large, which increased the G/W flow rate and exergy destruction. For the hybrid system, the G/W flow rate was reduced by increasing the temperature of the LNG through heat exchange with ammonia before vaporization, and the sum of the exergy destruction of the LNG-LNH_3 HEX and LNG-G/W HEX was reduced by 16% compared with the conventional system. In addition, the exergy efficiency of the LNG-G/W HEX and LNH_3-G/W HEX, where the fuel and G/W exchanged heat of the hybrid system, increased by 20% and 12.5%, respectively, compared with the independent system.

Table 7 presents the exergy destruction and efficiency of the mixer, tee, and RE-CONDENSER of the hybrid system. In the mixer and RE-CONDENSER, the exergy destruction increased as the temperature difference between the fluids in the inlet stream increased. Further, the exergy destruction of the mixer in the independent system was almost zero because the two introduced fluids were in similar states. In contrast, the RE-CONDENSER of the hybrid system experienced exergy destruction because of the significant temperature difference caused by the influx of BOG and LNG, and MIX 01 experienced exergy destruction because the fractioned LNG at different temperatures was remixed.

4. Conclusions

A hybrid fuel supply system for dual-fuel engines using LNG and ammonia was developed, and the operating pressure of the re-condensing system was determined as a process variable. The power consumption and SPC of the independent and hybrid systems were analyzed for engine load. The systems were evaluated by an exergy analysis of the equipment components and the entire system.

The optimal operating pressure for completely re-condensing the BOG_{LNG} in the hybrid system increased as the engine load decreased and the amount of ammonia increased.

The power consumption of the hybrid system was lower than that of the independent system, which indicates that it is more efficient to re-condense the BOG using cold energy within the system than to compress the BOG generated in the tank and use it directly as fuel.

For the independent system, the power consumption was determined by the power of the BOG compressor, which is not affected by the engine load and exhibits the opposite trend to the SPC. In contrast, for the hybrid system, the trends in the overall power consumption and SPC were similar because the hybrid system is significantly affected by the re-condensing system.

Compared with the independent system, the total exergy destruction of the hybrid system components was lower, and the exergy efficiency was higher. The heat exchanger for both systems was the highest exergy destruction equipment. Thus, additional research is required on the process variables affecting the heat exchanger's exergy destruction.

The economic analysis could not be performed because it was difficult to estimate the cost of ammonia-related equipment. The LNG and NH3 mixing ratio considered in this study may differ from the actual mixing ratio if the specifications of the applied engine are revealed. A techno-economic assessment combining thermodynamic analysis with economic analysis will be conducted in the future. Additionally, an appropriate method for handling NOx is required because NOx is generated when ammonia is used as fuel.

Author Contributions: Conceptualization, S.H.; methodology, S.H.; software, S.H.; validation, J.L. and S.H.; formal analysis, J.L.; investigation, S.H.; resources, S.H.; data curation, S.H.; writing—original draft preparation, S.H.; writing—review and editing, J.L. and S.H.; visualization, S.H.; supervision, J.C.; project administration, J.C.; funding acquisition, J.C. All authors have read and agreed to the published version of the manuscript.

Institutional Review Board Statement: Not applicable.

Informed Consent Statement: Not applicable.

Data Availability Statement: Not applicable.

Conflicts of Interest: The authors declare no conflict of interest.

Nomenclature

$\dot{m}$	mass flow rate kg/h
$\dot{E}_x$	Physical flow exergy kW
$\dot{E}_{x_{in}}$	Physical flow exergy of system inlet kW
$\dot{E}_{x_{out}}$	Physical flow exergy of system outlet kW
$\dot{e}_x$	mass exergy kJ/kg
T	temperature K
h	enthalpy kJ/kg
s	entropy kJ/kg
$\dot{Q}$	heat flow kW
$\dot{W}_{in}$	Work input kW

References

1. IMO Home Page. Available online: https://www.imo.org/en/MediaCentre/PressBriefings/pages/DecadeOfGHGAction.aspx (accessed on 20 May 2022).
2. Kim, D.; Lee, K.; Kwon, D. Trends of Cleaner Alternative Marine Fuels and Exhaust Emission Abatement Technology for Carbon Neutrality. *KIC News* **2022**, *2*, 2:1–2:20.
3. Burel, F.; Taccani, R.; Zuliani, N. Improving sustainability of maritime transport through utilization of Liquefied Natural Gas (LNG) for propulsion. *Energy* **2013**, *57*, 412–420. [CrossRef]
4. Park, C.; Kim, Y.; Choi, Y.; Lee, J.; Lim, B. The effect of engine speed and cylinder-to-cylinder variations on backfire in a hydrogen-fueled internal combustion engine. *Int. J. Hydrogen Energy* **2019**, *44*, 22223–22230.
5. Wijayanta, A.T.; Oda, T.; Purnomo, C.W.; Kashiwage, T.; Aziz, M. Liquid hydrogen, methylcyclohexane, and ammonia as potential hydrogen storage: Comparison review. *Int. J. Hydrogen Energy* **2019**, *44*, 15026–15044.
6. Fadhil, Y.; Mahmoud, M.; Margaux, M.; Rasmus, B. Renewalbe ammonia as an alternative fuel for the shipping industry. *Curr. Opin. Chem. Eng.* **2021**, *31*, 100670.
7. Zamfirescu, C.; Dincer, I. Using ammonia as a sustainable fuel. *J. Power Sources* **2008**, *185*, 459–465.
8. Reiter, A.J.; Kong, S. Demonstration of compression-ignition engine combustion using ammonia in reducing greenhouse gas emissions. *Energy Fuels* **2008**, *22*, 2962–2971. [CrossRef]
9. Uchida, M.; Ito, S.; Suda, T.; Fujimori, T. Performance of Ammonia/Natural Gas Co-Fired Gas Turbine with Two-Stage Combustor. In Proceedings of the AIChE 2019, Hyatt Regency, Orlando, FL, USA, 10–15 November 2019.
10. MAN Energy Solutions Home Page. Available online: https://www.man-es.com/docs/default-source/document-sync/man-b-w-two-stroke-engine-operating-on-ammonia-eng.pdf?sfvrsn=c4bb6fea_0 (accessed on 5 May 2022).
11. Dalian Shipbuilding Industry Company Home Page. Available online: https://wwwcdn.imo.org/localresources/en/OurWork/Environment/Documents/Symposium%202021/Presentations/First%20day%20-%20Blocks%201%20and%202/Symposium%20presentations%20-%20First%20Day/Block%202.1%20-%20Peng%20Guisheng_Green%20Technology%20Development-Ammonia%20Fuel.pdf (accessed on 5 May 2022).
12. Oh, S.; Park, C.; Kim, S.; Kim, Y.; Choi, Y.; Kim, C. Natural gas-ammonia dual-fuel combustion in spark-ignited engine with various air-fuel ratios and split ratios of ammonia under part load condition. *Fuel* **2021**, *290*, 120095:1–120095:11. [CrossRef]
13. Reiter, A.J.; Kong, S. Combustion and emissions characteristics of compression-ignition engine using dual ammonia-diesel fuel. *Fuel* **2011**, *90*, 87–97. [CrossRef]
14. Seo, S.; Chu, B.; Noh, Y.; Jang, W.; Lee, S.; Seo, Y.; Chang, D. An economic evaluation of operating expenditures for LNG fuel gas supply systems onboard ocean-going ships considering availability. *Ships Offshore Struct.* **2016**, *11*, 213–223. [CrossRef]
15. Seo, S.; Han, S.; Lee, S.; Chang, D. A pump-free boosting system and its application to liquefied natural gas supply for large ships. *Energy* **2016**, *105*, 70–79. [CrossRef]
16. Lee, Y.; Kim, Y.; Kang, H. An analysis on the characteristics of regasification system for gas fuelled ship depending on the mixing ratio of eglycol and water. *J. Korean Soc. Mar. Eng.* **2014**, *38*, 799–805.
17. Wang, C.; Ju, Y.; Fu, Y. Comparative life cycle cost analysis of low pressure fuel gas supply systems for LNG fueled ships. *Energy* **2021**, *218*, 119541:1–119541:9. [CrossRef]
18. Kim, D.; Hwang, D.; Gundersen, T.; Lim, Y. Process design and economic optimization of boil-offgas re-liquefaction systems for LNG carriers. *Energy* **2019**, *173*, 1119–1129. [CrossRef]

19. Gaztransport & Technigaz SA Home Page. Available online: https://gtt.fr/technologies/markiii-systems (accessed on 9 May 2022).
20. Gosiewski, K.; Pawlaczyk, A.; Warmuzinski, K.; Jaschik, M. A study on thermal combustion of lean methane-air mixtures: Simplified reaction mechanism and kinetic equations. *Chem. Eng. J.* **2009**, *154*, 9–16. [CrossRef]
21. Kulitsa, M.; Wood, D.A. Enhanced application for FSRU recondensing equipment during periods of low or no gas send out to minimize LNG cargo losses. *Petroleum* **2018**, *4*, 365–374. [CrossRef]
22. Cho, W.; Lee, H.; Ryu, B.; Kang, H. Design and assessment of reliquefaction system according to boil off gas reliquefaction rate of liquefied hydrogen carrier. *J. Navig. Port Res.* **2020**, *44*, 283–290.
23. Tsatsaronis, G. Definitions and nomenclature in exergy analysis and exergoeconomics. *Energy* **2007**, *32*, 249–253. [CrossRef]
24. Choi, J. Development of partial liquefaction system for liquefied natural gas carrier application using exergy analysis. *Int. J. Nav. Archit. Ocean Eng.* **2018**, *10*, 609–616. [CrossRef]
25. Li, Y.; Jia, M.; Kokjohn, S.L.; Chang, Y.; Reitz, R.D. Comprehensive analysis of exergy destruction sources in different engine combustion regimes. *Energy* **2018**, *149*, 697–708. [CrossRef]